

# DESIGN STUDY OF THE CEPC BOOSTER

C. Zhang, IHEP, CAS, P.O.Box 918, Beijing 100049, China

## Abstract

Design study of the CEPC booster is reported. The booster provides 120 GeV beams for the collider with top-up injection frequency of 0.1 Hz. To save cost, energy of the linac injector for the booster is chosen as 6GeV, corresponding to the magnetic field of 30 Gs. In this paper, lattice of the booster is described; the low injection energy issues are studied; beam transfer from linac to booster and from booster to collider are discussed.

## GENERAL DESCRIPTION

Soon after discovery of the Higgs boson, the Circular Electron-Positron Collider (CEPC) was proposed. The Super Proton-Proton Collider (SPPC) could be installed later in the same tunnel of CEPC for  $e^+e^-$ , pp, ep and ion collisions [1].

The booster is in the same tunnel of the collider with about same circumference, while bypasses are arranged to keep away from detectors in IP1 and IP3. Electron and positron beams are injected from the linac to the booster through the transfer line LTB (Linac To Booster) in one of the 850 m long straight sections. The beam extraction at top energy takes place in other two straight sections. Electron and positron beams are injected to the collider through BTCE<sup>+</sup> and BTCE<sup>-</sup> (Booster To Collider) transfer lines. Figure 1 illustrates the layout of the booster on the upside of the CEPC collider.

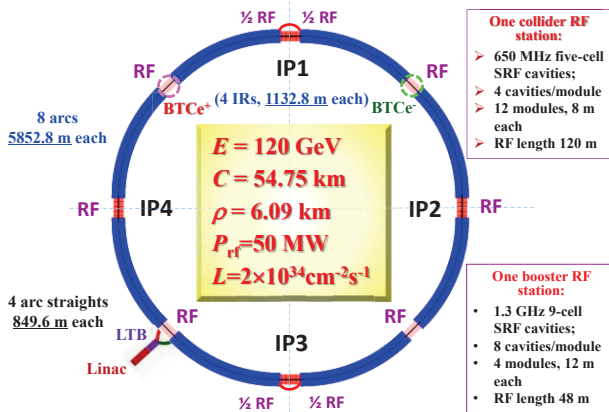


Figure 1: Layout of CEPC and its booster.

As shown in Fig.1, the collider is designed with four interaction points, where IP1 and IP2 are for  $e^+e^-$  collisions of luminosity  $2 \times 10^{34} \text{ cm}^{-2} \text{ s}^{-1}$  each, while other two IP's are reserved for future pp collider SPPC. The circumference of CEPC collider is 54.75 km, including 8 arcs of 5852.8m, 4 arc straights of 849.6 m each and 4 interaction region straights of 1132.8 m each. The RF frequency of the booster is chosen as 1.3 GHz, factor of two higher than that in the collider. There are eight RF stations in the booster, providing total RF voltage of 5.12 GV. One RF station consists of 4 cry-modules of 12 m long each, each of them

contains eight 9-cell super-conducting cavities. Table 1 lists the main parameters of the CEPC booster.

Table 1: Main Parameters of the CEPC Booster

Parameter	Unit	Value	
Injection energy	GeV	6	
Ejection energy	GeV	120	
Circumference	km	52.75	
Bending radius	km	6.519	
Bending field	@ 6 GeV	T	0.0614
	@ 120 GeV		0.00307
SR loss/turn	GeV	2.814	
Bunch number		50	
Bunch population	$10^{10}$	2.0	
Beam current	mA	0.87	
RF frequency	GHz	1.3	
Total RF voltage	GV	5.12	
SR power @ 120GeV	MW	2.46	
SR power density @120GeV	W/m	45	

The bunch number in the booster is chosen the same as in the collider. The bunch population is based on the assumption of 5% current decay in the collider between two top-ups. Synchrotron radiation power density of 45W/m at 120 GeV in CEPC booster is much lower than in BEPCII of 415W/m [2].

For the very low synchrotron radiation damping rate, a scheme of single bunch injection from linac to booster is adopted. The electron and positron beams with bunch population of  $2 \times 10^{10}$  and emittance of 0.3 mm-mrad are injected into central orbit of the booster. Overall transfer efficiency from linac to the collider is assumed to be 90 %.

The booster operates with a repetition frequency of 0.1 Hz, the typical magnetic cycle is given in Fig. 2. Shown in Fig.2, the beam injection from the linac to the booster takes 1 second, the energy ramp takes 4 seconds, 1 second flat top is for beam extraction to the collider, and 4 seconds for magnets ramping down.

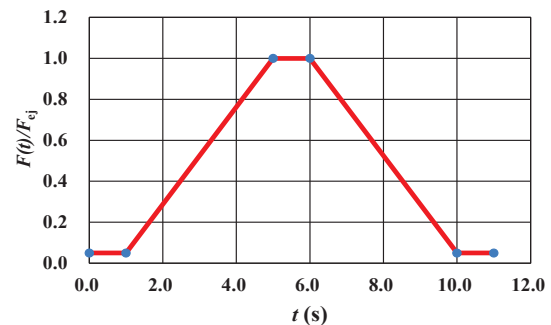


Figure 2: Typical magnetic cycle in the booster.

## LATTICE

### Choice of Cell Length

For the booster is installed in the CEPC tunnel, its arc arrangement should be similar to the collider. However, the length of the cells can be optimized with required beam property and other parameters in order to improve cost performance. Lattice parameters scaling to the cell length are presented in Table 2.

Table 2: Lattice Parameters Scaling to the Cell Length

Parameter	Value			Unit
$L_{\text{cell}}$	47.2	71.7	94.4	m
$ k_{Q Q}  \propto L^{-1}$	0.044	0.029	0.022	$\text{m}^{-1}$
$\beta_{\text{max}} \propto L$	81.2	123.3	162.3	m
$D_x \propto L^2$	0.38	0.87	1.52	m
$\nu_{x,y} \propto L^{-1}$	189.2	124.6	94.6	
$\alpha_p \propto L^2$	3.43	7.91	13.72	$10^{-5}$
$\xi \propto L^{-1}$	86.4	56.9	43.2	
$ k_{\text{SF}}  \propto L^{-3}$	0.15	0.043	0.019	$\text{m}^{-2}$
$ k_{\text{SD}}  \propto L^{-3}$	0.24	0.070	0.030	$\text{m}^{-2}$
$\varepsilon_{x0} \propto L^3$	6.8	23.8	54.40	nm
$\nu_s \propto L$	0.204	0.31	0.41	
$\sigma_{x\beta} \propto L^2$	0.74	1.71	2.97	mm
$\sigma_{y\beta} \propto L^2$	0.53	1.21	2.10	mm
$\sigma_{xE} \propto L^2$	0.49	1.14	1.97	mm
$\sigma_x \propto L^2$	0.89	2.06	3.57	mm
$\sigma_z \propto L$	1.84	2.76	3.68	mm

It is indicated in Table 2 that longer the cell, the larger the beta functions, dispersion, emittance and beam size, and also smaller the chromaticity, weaker the sextuples, and, more importantly, the less cell number and machine components. The cell length of the booster is then chosen as 71.7m, about 1.5 times of the collider of 47.2 m, as the baseline design. The total FODO cells in the booster is 764.

### Lattice Functions

The lattice of the booster is based on 60° FODO cells. The structure of two types of super-periods in the booster is indicated in Fig.3.



Figure 3: Layout of CEPC and its booster.

There are 8 arcs in the booster, each of them consists of 78 FODO cells and two dispersion suppressors (each contains one regular FODO cell and one straight FODO

cell). There are two quadrupoles of 1 m each, 8 dipoles of 8 m each, two sextupoles of 0.2 m each in a regular FODO cell of 71.7 m. Total length of an arc is 5846.6 m. There are 12 straight FODO cells in the arc straight and 15 straight FODO cells in the IR straight (for IR2 and IR4). In IR1 and IR3, two bypasses are designed to keep away from the detectors. The computer code MAD [3] is applied for the optics design. The lattice functions in the booster are shown in Fig. 4.

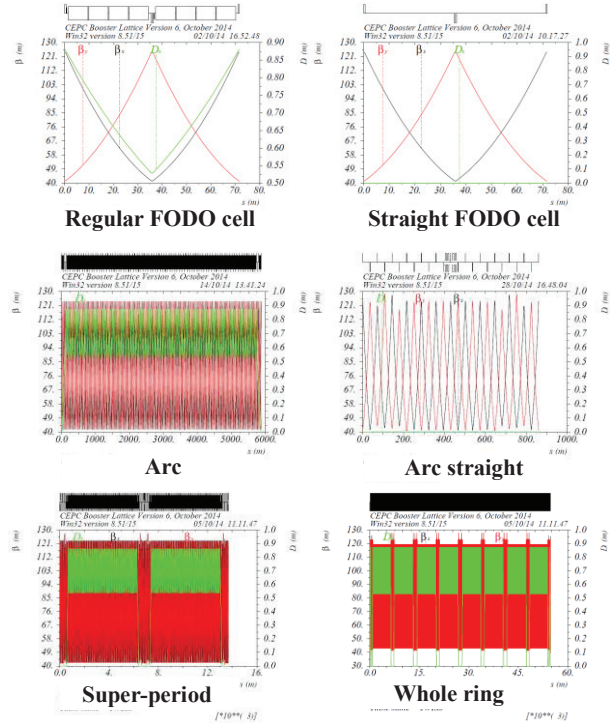


Figure 4: Lattice functions in the booster.

### Bypasses

Two bypasses are arranged in the booster to make the beamline skirting the detectors at IP1 and IP3 of the collider. The structure of a half bypass is shown in Fig. 5.

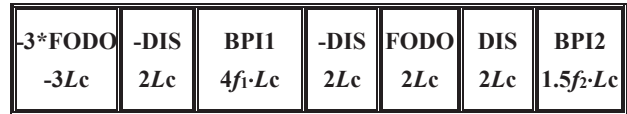


Figure 5: Structure of half bypass.

Seen in Fig.5 the bypasses are also based on FODO cells. The idea of the booster bypass design is to move out 3 regular FODO cells in arcs to the bypasses and keep the straight sections BPI1 and BPI2 dispersion free. The advantage of this design is that no additional bending magnet is required. The length of a bypass is  $L_{\text{bp}} = 2 \times (6 + 4f_1 + 1.5f_2) \cdot L_c$  and the width of the bypass is  $W_{\text{bp}} = (9.5 + 9f_1) \cdot \theta_c \cdot L_c$ . By properly choosing the factors  $f_1$  and  $f_2$ , both length and width of bypasses can be adjusted to meet the length of interaction region and detector width. In present design, we take  $f_1 = 1.0$  and  $f_2 = 1.0$  making bypass width of 13.0m and total length of  $2 \times 820$  m, and the circumference about the same as the collider.

Lattice functions in long straights in IP2 & IP4 and half bypass in IP1 & IP3 are shown in Fig. 6.

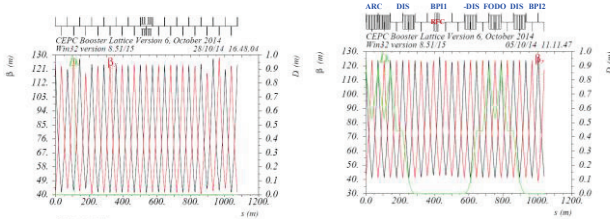


Figure 6: Lattice functions in long straights in IP2 & IP4 and half bypass in IP1 & IP3.

**Dynamic Aperture**

Dynamic aperture of the booster is studied with optics computing code SAD [4]. Two family of sextupoles SF and SD near quadrupoles QF and QD in FODO cells are used for chromaticity correction with corrected  $\xi_x = \xi_y = 0.5$ . Figure 7 plots the dynamic aperture for particles of  $\Delta p/p = 0, \pm 1\%, \pm 2\%$  by tracking of 3 damping times assuming the transverse coupling  $r = \epsilon_y/\epsilon_x = 0.01$ .

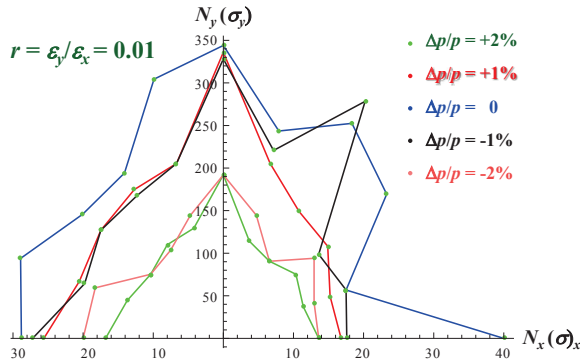


Figure 7: Dynamic aperture plot.

As a summary of this section, the lattice related parameters of the booster are given in Table 3.

Table 3: Lattice Parameters of the Booster

Parameter	Unit	Value
FODO cell length	m	71.665
Total number of FODO cells		764
Phase advance in a cell (H/V)		60°/60°
Length of D/Q/S magnets	m	8.0/1.0/0.2
Maximum $\beta$ function (H/V)	m	123.8/123.0
Transverse betatron tune (H/V)		127.2/127.3
Maximum dispersion function	m	0.879
Length of bypass	m	1640
Width of bypass	m	13.0
Emittance (H/V)	nm-rad	20.5/0.205
Damping time (Trans./Long.)	ms	15.6/7.8
Momentum compaction factor	$10^{-5}$	7.69
Beam energy spread	%	0.127
Synchrotron oscillation tune		0.32076
Bunch length ( $V_{rf}=5.12$ GV)	mm	2.66
Maximum beam size (H/V)	mm	1.948/0.159

**LOW INJECTION ENERGY ISSUES**

It is seen in Table 1, the bending field of CEPC booster is 614Gs at 120 GeV. To reduce the cost of linac injector, the injection beam energy for booster is chosen as low as 6 GeV with the magnetic field as low as 30.7 Gs, about 1/7 of the injection field of LEP [5]. The question is if the magnetic field is stable enough at such a low field against the earth field of 0.5-0.6 Gs and its variation. To mitigate the low field problem, effort is also made to increase the bending field at injection with the proposed wiggling band scheme. Moreover, the beam instability at 6 GeV is discussed.

**Low Field Stability Test**

Taking advantage of the existing BEPC bending magnet and power supply, low magnetic field stability was tested. The stability of the power supply is better than  $1 \times 10^{-4}$ . A Hall probe system is used for field measurement with accuracy of 0.1Gs or  $\Delta B/B$  of  $3 \times 10^{-3}$ . The setup for the test is shown in Figure 8.



Figure 8: The magnetic field test setup.

The test was performed by IHEP magnet group [6]. The magnetic field outside and inside of the magnet with zero excitation current was measured first. As shown in Figure 9, the earth field (outside the magnet) is about 0.8 Gs, with  $B_x=0.55$  Gs (south-to-north),  $B_y=0.45$  Gs (vertical) and  $B_z=0.25$ Gs (east-west); while the field inside the magnet is dominated by its residual field.

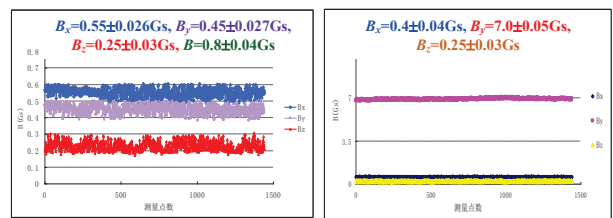


Figure 9: Measured field outside & inside of the magnet.

The 24-hour magnetic field stability was measured for different excitation currents, given in Figure 10.

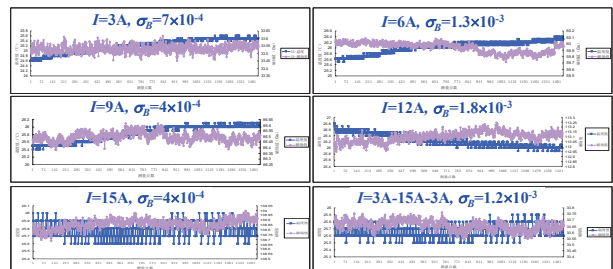


Figure 10: 24-hour magnetic field stability test for different excitation currents.

The test shows that the magnetic field stability around 30 Gs is about  $1 \times 10^{-3}$ , which indicates the injected beam energy for booster of 6 GeV could be feasible in view of field stability.

*Low Field Stability Test*

The idea of wiggling bend scheme comes from wiggler magnets applied in synchrotron radiation facilities that higher field cancelation makes zero or lower integrated field. The proposed scheme is shown in Figure 11. There are four bending magnets in half cell of the booster, two outside bends are excited by a bipolar power supply making the wiggling bands so that the operating magnetic field gets higher.

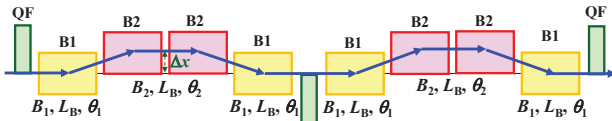


Figure 11: The magnetic field test setup.

The magnetic field of the bending magnets is properly set during energy ramp to keep total bending angle constant, i.e.  $\theta_{B2} + \theta_{B1} = 2\theta_B$ . In principle, the oppositely excited bends  $B_1$  can be as low as  $-0.9B_{ej}$  at injection for  $B_2 = B_{ej}$ . However, the orbit offset  $\Delta x = \theta_1 \times (L_B + L_D)$  may get too large, where  $L_B$  and  $L_D$  are length of bending magnets and the drift space between the magnets. Here we take  $B_1 = -0.1B_{ej} = 60\text{Gs}$ , and  $B_2 = 0.2B_{ej}$ , i.e. double the magnetic field of the baseline design with  $\Delta x = 20\text{ mm}$ . Magnetic field and energy ramping curves are given in Fig.12.

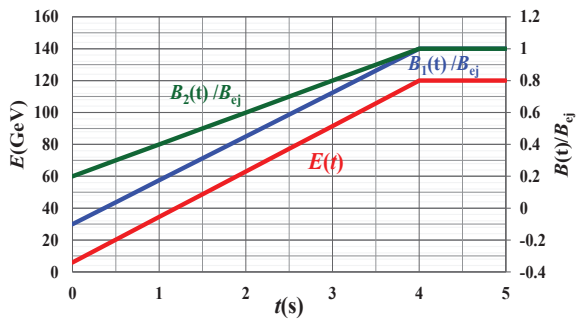


Figure 12: Magnetic field and energy ramping curves in wiggling bend scheme.

*Instability Issue*

The low injection energy not only results in the low magnetic field, but also beam instability. The beam energy in the booster at injection is 1/20 of that in the collider, while the beam intensity in the booster is also 1/20 of the collider. However, beams may get unstable for almost no synchrotron radiation damping in the booster. The special concern is on transverse mode coupling instability, coupled bunch instability excited by high order modes in 1.3 GHz superconducting cavities and resistive wall effect. Study on beam instability in the booster is in progress. In any case, bunch-by-bunch feedback system should be equipped in the booster to provide damping mechanism in order to stabilize beams.

**BEAM TRANSFER**

6 GeV electron and positron beams from the linac are injected into the booster ring through the transfer line LTB, accelerated to the top energy of 120 GeV and then extracted to the collider through the transfer line BTC.

*Beam Transfer from Linac to Booster*

The function of the transfer line LTB is to bring electron and positron beams from the linac to booster and to match to its phase space functions. The layout of LTB is illustrated in Fig. 13.

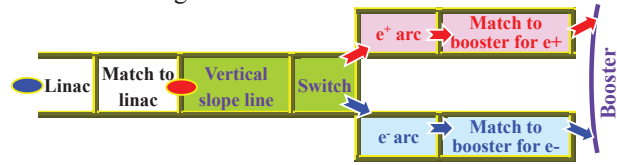


Figure 13: Layout of beam transfer line LTB.

As shown in Fig. 13, the transfer line LTB is comprised of a vertical slope line (VSL), a switch yard and  $e^+e^-$  branch lines. The vertical slope line connects the linac of ground level to the booster of 50 m deep. It consists of a bend down section making a 1:10 slope, successive 15 straight  $90^\circ$  FODO cells and a bend down section making dispersion free at the end of VSL. The switch yard matches the Twiss parameters with VSL and delivers electron and positron beams to their individual branch lines. In the  $e^+$  and  $e^-$  branch lines, beams are transferred in two arcs and then matched to the booster through the final matching sections. Each arc contains 2 dispersion suppressors and 6 regular  $90^\circ$  FODO cells. The dispersion suppressors are carefully arranged to avoid conflict of the magnets in two branches. The lattice functions in the transfer line LTB are shown in Fig. 14.

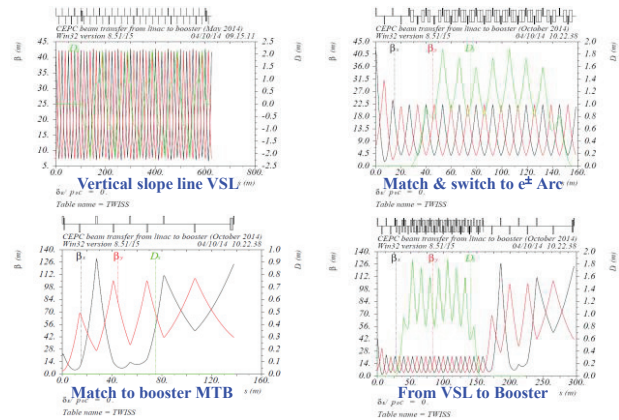


Figure 14: The lattice functions in the transfer line LTB.

*Beam Injection to Booster*

Through the transfer line LTB, electron and positron beams are injected into the booster from outside of the ring. Horizontal septum is used to bend beams into the booster, and a single kicker downstream of injected beams kicks the beams to the booster orbit with maximum injection rate of 100 Hz. Figure 15 pictures the injecting bunch in the septum and the injected bunch in the booster. The kicker

needs to deflect the beam with displacement of  $x_k=12\sigma_{x,ej}+3\sigma_{x,inj}+d$  at the entrance of the septum in order to avoid particle loss of both injecting and injected bunches.

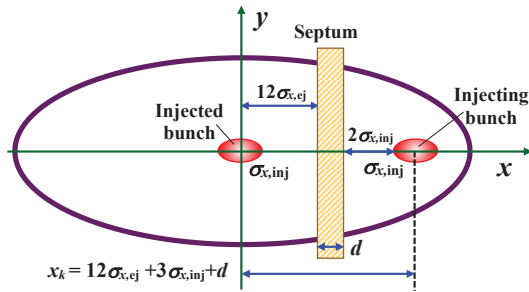


Figure 15: Injecting and injected bunches at entrance of septum.

Main parameters of the injection septum and kicker are listed in Table 4. The strength of the septum and the kicker corresponds to the energy of 12 GeV for future upgrade.

Table 4: Main Parameters of the Injection Septum and Kickers

Magnet type	Length (m)	$\theta$ (mrad)	Field (T)	Aperture	
				H (mm)	V (mm)
Septum	2.0	9.1	0.18	41.4	13.4
Kicker	0.5	0.40	0.032	41.4	13.4

*Beam Extraction From Booster*

Single kicker and 4 orbit bumps are used for beam extraction horizontally from the booster with maximum extraction rate of 100 Hz. A Lamberstson magnet is applied to bend beams vertically into the transfer line BTC. Main parameters of the extraction septum and kicker are listed in Table 5.

Table 5: Main Parameters of the Injection Septum and Kickers

Magnet type	Length (m)	$\theta$ (mrad)	Field (T)	Aperture	
				H (mm)	V (mm)
Septum	10.0	9.1	0.41	41.4	18.6
Kicker	2.0	0.33	0.046	41.4	13.6

*Beam Extraction from Booster*

The booster is mounted in the CEPC tunnel 2m above the collider. The Lamberstson septum bends beams down to the transfer line BTC. Beams are transferred and

matches their Twiss parameters to the collider in BTC. Detail BTC design needs to be carried out together with collider injection. The lattice functions in BTC are shown in Fig. 16.

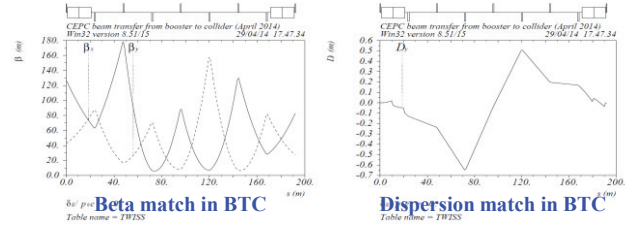


Figure 16: Lattice functions in the transfer line BTC.

**SUMMARY**

The pre-conception design study on CEPC booster described in above sections finds no showstopper in view point of lattice, bypasses, dynamic aperture, beam transfer and requirement to technical systems. The issues related to the low energy injection, including the low magnetic field performance and beam instabilities, remain a central concern in the design. The wiggling bend scheme is proposed to mitigate this problem, while schemes of extending the linac injector with damping rings and adding a pre-booster are being considered. There are some technical challenges, such as the low HOM 1.3 GHz SC cavities, supports & alignment, as well as low cost components. The design study needs to be detailed and deepened.

**ACKNOWLEDGMENT**

The author would like to thank all members of the CEPC design team for their perfect collaboration.

**REFERENCES**

- [1] Q.Qin, Overview of the CEPC Accelerators, HF2014 proceedings, THP3H2.
- [2] BEPCII Team, Performance and Prospects of BEPCII, Proc. IPAC2012, 1030-1034, May 2012.
- [3] H. Grote, C. Iselin, The MAD Program User's Reference Manual, CERN/SL/90-13(AP).
- [4] SAD Home Page, Strategic Accelerator Design, <http://acc-physics.kek.jp/SAD/>.
- [5] LEP Design Report, CERN-LEP/TH/83-29, June 1983.
- [6] Z. Zhang, Low field stability test of the BEPC dipole, IHEP Internal Report, June, 2014.